Applied Surface Science 349 (2015) 833–838

Contents lists available at ScienceDirect

Applied Surface Science

journal homepage: www.elsevier.com/locate/apsusc

Surface activation of carbon paper with potassium dichromate lotion and application as a supercapacitor

Zhiyu Cheng, Peng Liu, Bing Guo, Yongfu Qiu*, Pingru Xu, Hongbo Fan*

College of Chemistry and Environmental Engineering, Guangdong Engineering and Technology Research Center for Advanced Nanomaterials, Dongguan University of Technology, Guangdong 523808, PR China

ARTICLE INFO

Article history:
Received 21 January 2015
Received in revised form 13 May 2015
Accepted 14 May 2015
Available online 21 May 2015

Keywords:
Supercapacitor
Carbon paper
Potassium dichromate lotion
Nanomaterials

ABSTRACT

In this paper, an effective strategy using potassium dichromate lotion to activate surfaces of commercial carbon papers leading to enhanced electrochemical capacitances was reported. It is revealed that surfaces of activated carbon papers became rougher and their specific surface areas enlarged after treatment. Further, surface hydrophilicity of the treated carbon papers enhanced due to the generation of hydrophilic groups such as hydroxyl (–OH), carbonyl (C=O) and carboxyl (–COOH) and they act as strong polar sites to absorb water molecules. With the synergistic effect of enlarged specific surface area and enhanced surface hydrophilicity, the activated carbon papers provide high areal capacitances. In general, this strategy offers a feasible pathway to make commercial carbon paper a promising candidate for practical supercapacitors and is expected to extend to other carbon based electrode materials.

1. Introduction

Supercapacitors (SC) as one of the most promising energy-storage devices, have drawn great research interests because of their outstanding electrochemical behaviours, such as high power density, excellent stability, light-weight and ease to handle [1–9]. Various forms of carbon-based materials, especially carbon nanotubes and graphene, with large electrochemically accessible surface area, appropriate pore size and distribution, continuous pathways for rapid ion transport, large electrical conductivity and good wettability, have been considered as promising candidates for electrodes in supercapacitors [1–3]. Comparing to carbon nanotubes and graphene, carbon paper (CP) holds great prospect as an electrode material for SC since it is inexpensive and highly conductive [10]. However, it usually has a lower specific surface area and accordingly a relatively lower specific capacitance (1–2 F/g) [11] in comparison with that of graphene (100–200 F/g) [12] and single-walled carbon nanotubes (100–200 F/g) [13]. Herein, an effective strategy is developed to increase specific surface area of commercial carbon paper, improve its hydrophilicity and accordingly enhance its electrochemical capacitance as electrodes in supercapacitors.

2. Experimental

2.1. Preparation of activated carbon paper (ACP):

Carbon papers (1.0 cm × 5.0 cm, the mass density is 31 mg/cm^2, purchased from Jixing Sheng'an company) were immersed in a solution containing 20.0 mL of concentrated H_2SO_4 (98%) and 2.0 g of $K_2Cr_2O_7$ (slowly added into H_2SO_4) at 25 °C for controlled periods of time (10, 60, and 120 s). Taken out and washed with distilled water for several times, the activated carbon papers were heated at 150 °C for 2 h. Samples treated for different time (10, 60, 120 s) were denoted as ACP-10, ACP-60 and ACP-120, respectively.

2.2. Characterization

The morphologies of treated and untreated carbon papers were characterized by Scanning Electron Microscopy (SEM) using JEOL 6701F at an accelerating voltage of 5 kV. The specific surface areas of samples were determined by nitrogen adsorption at 77 K with a JWGB SCI. & TECH BK132F automatic adsorption apparatus; Attenuated Total Reflectance Fourier Transform Infrared Spectroscopy (ATR-FTIR) were obtained on a Thermo Nicolet 6700 spectrometer; Contact angles were obtained from a surface tension meter (Dataphysics OCA20, Germany) at 25 °C. XPS spectra were obtained using a KRATOS AXIS ULTRA DLDXPS instrument equipped with a monochromatic Al K_a ($h\nu$ = 1486.6 eV) X-ray source. All of the XPS spectra were collected at a takeoff angle of 90°, with the path energy

* Corresponding author. Tel.: +86 769 2286 1232; fax: +86 769 2286 1232.
E-mail addresses: qiuyf1979@foxmail.com (Y. Qiu), fhb666666@126.com (H. Fan).

http://dx.doi.org/10.1016/j.apsusc.2015.05.086
0169-4332/

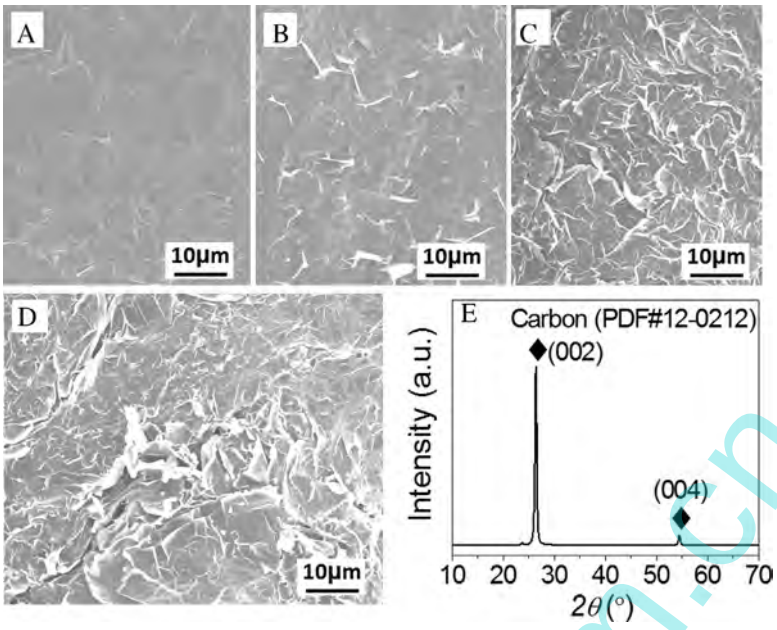

Fig. 1. SEM images of: (A) CP; (B) ACP-10; (C) ACP-60; (D) ACP-120; (E) XRD pattern of CP (A).

of the photoelectron analyzer at 40 keV and a step size of 0.1 eV. The atomic force microscope (AFM) image was taken on a scanning probe microscope (CSPM5600, Being Nano-Instruments LTD).

Cyclic voltammetry (CV) and galvanostatic charge/discharge measurements were performed in a three-electrode system using a CHI 440a electrochemical work station, with 1.0 M Na_2SO_4 as the electrolyte solution. Carbon papers with an area of 1.0 cm^2 were used as the working electrode, Ag/AgCl (3.0 M KCl) and a Pt wire were used as the reference and counter electrode, respectively. The electrochemical impedance spectroscopy (EIS) measurements were carried out by using a potentiostat (EG&G, M2273), the frequency range analyzed was 0.1–100 Hz with ac amplitude of 10 mV.

Calculation [14]: The areal capacitance for the electrode can be calculated as, $C = (1/(S\upsilon(U_c - U_a))) \int_{U_a}^{U_c} I(U)\,dU$, where C is the areal capacitance (F/cm^2), S is the projected area of the carbon paper (cm^2), υ is the potential scan rate (V/s), $U_c - U_a$ is the sweep potential range during (U) discharged and $I(U)$ denotes the response current density (A/cm^2). Gravimetric capacitance for a single electrode was calculated from the discharge curve in a three-electrode cell with the equation, $C_{single} = I\,\Delta t/(\Delta V \times S)$, where I, Δt, ΔV and S are the constant current, the discharge time, the voltage change during the discharge process and the projected area.

3. Results and discussion

3.1. SEM, XRD, and nitrogen-adsorption

The SEM images in Fig. 1 reveal the surface morphologies of ACP-10, ACP-60 and ACP-120, respectively. Their surfaces turned rougher with the increased treated time, as observed from Fig. 1A to D, which indicated that the surfaces of carbon papers were modified by potassium dichromate lotion. A XRD pattern for CP is shown in Fig. 1E, which is ascribed to carbon (PDF#12-0212) with lattice constants of a = 0.2464 nm and c = 0.6736 nm.

In order to examine the surface properties of ACP, AFM and nitrogen adsorption–desorption measurements were performed. AFM results in Fig. 2A shows that the surface of ACP-120 became Rugged. In Fig. 2B, both adsorption isotherms for CP and ACP-120 show a sharp increase near the relative pressure P/P_o of 1, indicating that only the macropores exist within the samples. Further, the specific surface areas for CP and ACP-120 calculated according to the Brunauner-Emmett-Teller (BET) analysis are 8.4 and 22.2 m^2/g, respectively. The specific surface area for ACP-120 is higher than that of CP, implying that potassium dichromate lotion corroded the surface and accordingly led to a larger specific surface area.

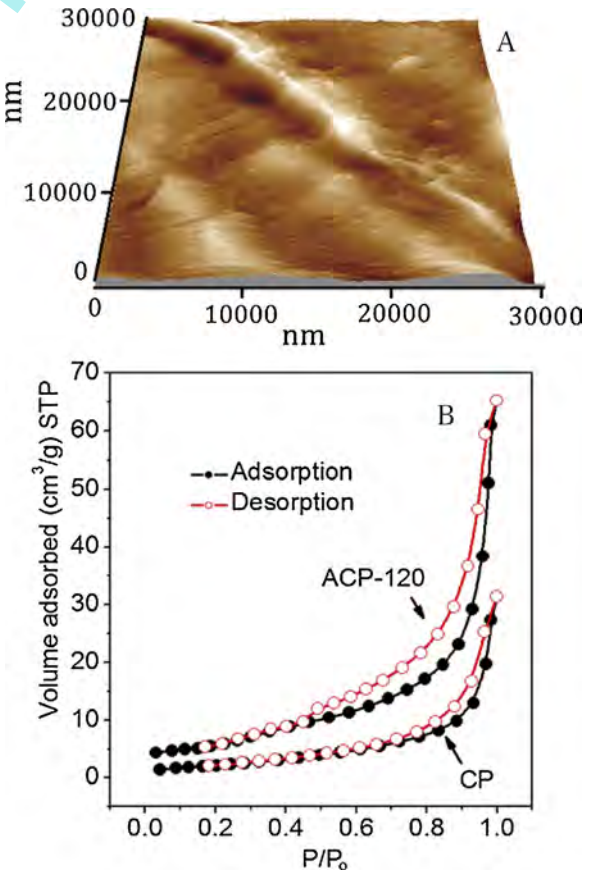

Fig. 2. (A) Three-dimension AFM image of ACP-120; (B) N_2 adsorption–desorption isotherms for CP and ACP-120.

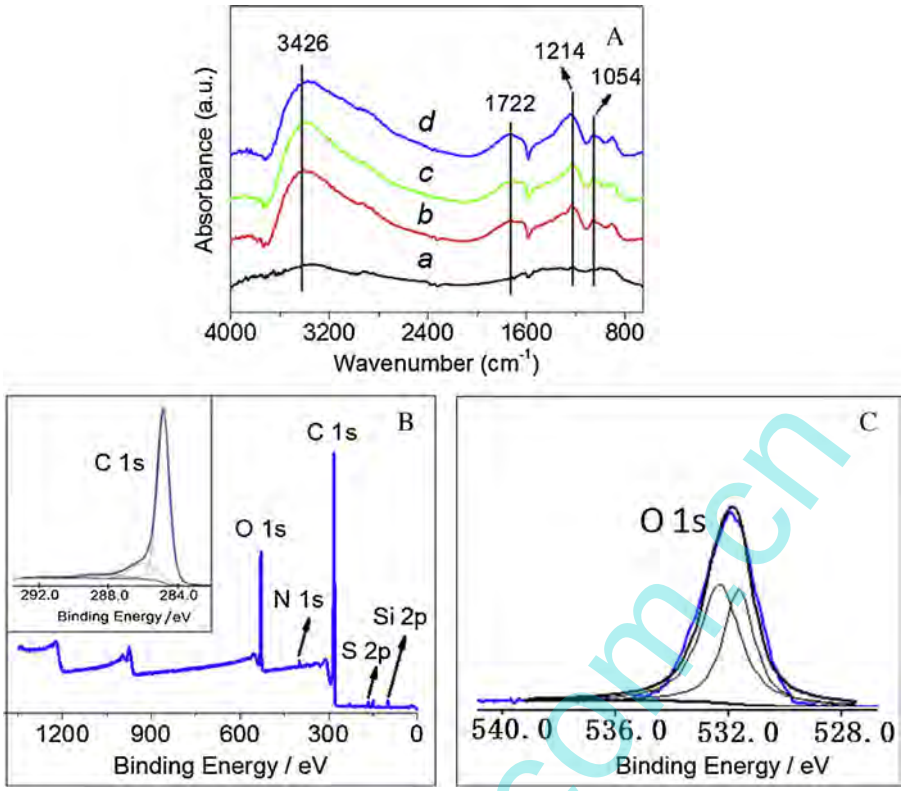

Fig. 3. (A) ATR-FTIR spectra recorded for: (a) CP; (b) ACP-10; (c) ACP-60; (d) ACP-120. (B) XPS spectrum in the whole energy range for ACP-120; inset in (B) is C 1s XPS spectra of ACP-120; (C) O 1s XPS spectra of ACP-120.

3.2. ATR-FTIR and XPS

In order to remove the adsorbed water, the samples were heated at 40 °C under vacuum for 24 h before ATR-FTIR measurements. The ATR-FTIR spectra of CP, ACP-10, ACP-60 and ACP-120 are shown in Fig. 3A. In general, the peaks at 1054, 1214, 1722 and 3426 cm^{-1} correspond to the stretching vibrations of C–O, C–H, C=O and –OH. [15–17] As for the CP, no peaks appear at 1054, 1722 and 3426 cm^{-1}, indicating that the groups of C–O, C=O and –OH were rarely found within untreated carbon paper. In contrast, the samples ACP-10, ACP-60 and ACP-120 obviously show peaks at 1054, 1214, 1722 and 3426 cm^{-1}, implying that groups of C–O, C–H, C=O and –OH were generated after oxidization treatment. The coexistence of –OH and C=O groups suggest that the –COOH groups have been successfully introduced on the surface of treated carbon papers [15].

In Fig. 3B the surface elements analysis was performed by the X-ray photoelectron spectra (XPS) for ACP-120 in wide energy range. The binding energy was determined by reference to C 1s line at 284.8 eV. Generally, elements C and O can be observed in ACP-120 and some impurities such as N, S and Si existing in the commercial carbon paper can also be detected. According to the equation, $C_O = (I_O/S_O)/(\sum_i I_i/S_i)$ the O concentration is calculated to be 18.2 atom%, where C_O is the oxygen concentration, I_O and I_i are the peak intensities of oxygen and other elements, S_O and S_i are the relative sensitivity factors of oxygen and other elements [18]. In order to determine the chemical states of the element C, core level XPS spectra of C 1s in ACP-120 have been obtained and shown in inset of Fig. 3B. Five binding energies 284.8, 285.9, 287.9, 289.6 and 291.6 eV can be observed, respectively. They are assigned to the carbons in functional groups of C–C, C–O–C, –C–OH, C=O, and O–C=O [19]. The core level XPS spectra of O 1s in ACP-120 have been shown in Fig. 3C. There are two binding energies 531.5 and 532.4 eV, which can be assigned to the oxygen in functional groups of O–C=O and C–O–C [20]. The XPS results further confirmed that the surface of the carbon paper has been oxidized and functionalized.

3.3. Wetting property

The wetting property of the carbon paper was characterized by water contact angle test [21]. In Fig. 4, descending contact angles for CP, ACP-10, ACP-60 and ACP-120 could be observed, implying that their surface hydrophilicity gradually enhanced via the potassium dichromate lotion treatment for longer time. The effect of surface roughness on the wetting behaviour has been explained by Söz [22] according to the equation, $\cos\theta_R = r \cdot f \cos\theta + f - 1$, where θ_R is the apparent contact angles measured on a rough surface, θ is the apparent contact angles measured on a smooth surface, r is

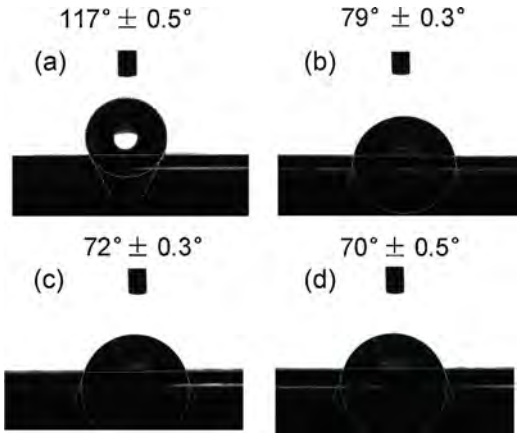

Fig. 4. Cross-sectional views of water droplets on: (a) CP; (b) ACP-10; (c) ACP-60; (d) ACP-120.

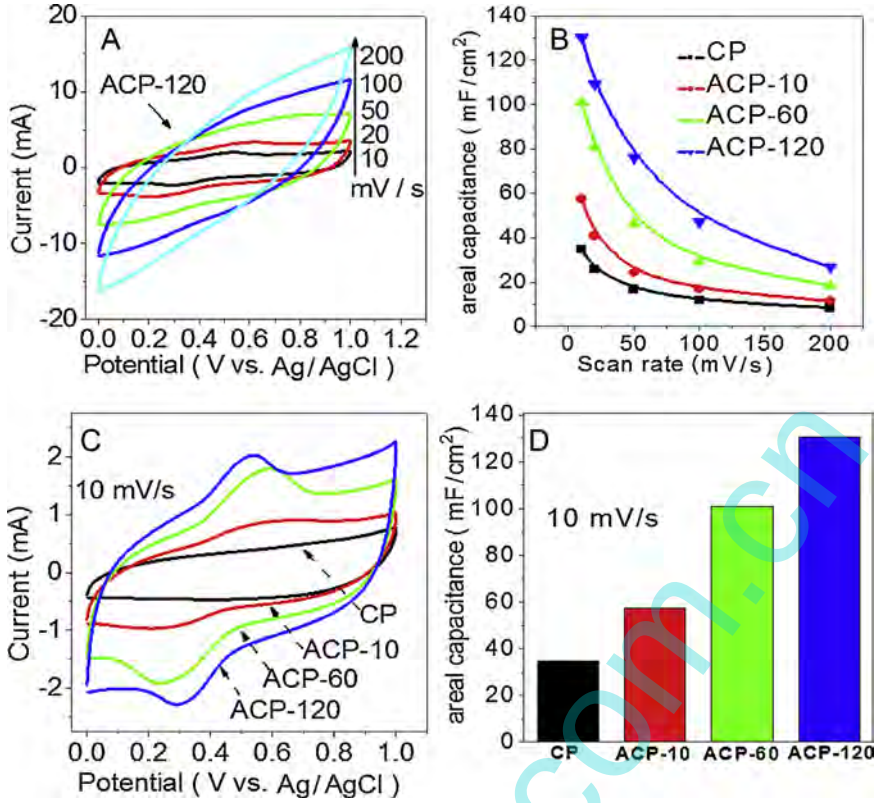

Fig. 5. (A) Cyclic voltammograms collected at different scan rates for ACP-120; (B) Calculated areal capacitances of the samples (CP, ACP-10, ACP-60, and ACP-120) from CV as a function of scan rate; (C) Enlarged CV diagrams for CP, ACP-10, ACP-60, and ACP-120 at scan rate 10 mV/s; (D) Calculated areal capacitances of the samples (CP, ACP-10, ACP-60, and ACP-120) at scan rate 10 mV/s.

defined as the ratio of the actual area of a rough surface to its projected geometric area and its value is always greater than 1, f is defined as the fraction of the surface on top of the protrusions. This indicates that the surface roughness would increase the apparent contact angles measured on a rough surface. However, for our cases, the enhancement of surface hydrophilicity leading to the apparent contact angles decreasing after treatment is due to hydroxyl (–OH), carbonyl (⟩C═O) and carboxyl (–COOH) groups generated on ACP and they are deemed to serve as strong polar sites to absorb water molecules [23].

3.4. Cyclic voltammetry (CV), galvanostatic charge/discharge and EIS

The typical CV curves for ACP-120 under different potential scan rates in Fig. 5A show that the areas of the CV curves increase with the increasing potential scan rates. Their areal capacitances calculated using $C = (1/S\upsilon(U_c - U_a)) \int_{U_a}^{U_c} I(U)\,dU$ [14] are shown in Fig. 6B. Obviously, fast decreases of the areal capacitances for ACP-120 can be observed as the potential scan rates increased from 10 to 200 mV/s. Comparing to other samples (CP, ACP-10 and ACP-60), ACP-120 has higher areal capacitances under different potential scan rates, implying that longer treatment time leads to advantages in electrochemical capacitances. Capacity retention as high as 36.1% for ACP-120 at a high scan rate 100 mV/s was observed, indicating its high rate capability. Interesting CV results for the samples ACP-10 ACP-60 and ACP-120 at scan rate 10 mV/s are shown in Fig. 6C. Clearly, a couple redox peaks for the ACP samples at 0.2–0.5 V could be observed. These two peaks are ascribed to the redox of function groups of C–O–C, –C–OH, C═O, and O–C═O on the surface of activated carbon paper [24]. Accordingly, no similar redox peaks are observed for the CP. As given in Fig. 6D, the calculated areal capacitances for the samples CP, ACP-10, ACP-60 and ACP-120 at scan rate 10 mV/s are 34.8, 58.3, 103.4 and 130.5 mF/cm^2. The increasing areal capacitances for samples with longer treatment time confirm that carbon papers treated by the potassium dichromate lotion for appropriate time own excellent capacitive characteristics. At a current density 10.0 A/g, the calculated specific capacitance for ACP-120 is 130.5 mF/cm^2. This value is much higher than 30.0 mF/cm^2 for the carbon materials electrode and lower than 460.0 mF/cm^2 for vertical grapheme electrodes [25]. It should be noted that the mechanical properties of activated carbon paper degraded quickly after 300 s of treatment time.

Capacitive responses of the samples were further probed using galvanostatic charge/discharge measurements in the three-electrode cell. In Fig. 6A, the charge–discharge curves at various current densities for ACP-120 generally show symmetrical and linear profiles, suggesting that the sample owns excellent capacitive behavior of typical double layer model. According to the equation $C_{single} = I\,\Delta t/(\Delta V \times S)$, the calculated areal capacitances for a single electrode are shown in Fig. 6B. When the current densities are 1, 2, 4, 6, 8 and 10 mA/cm^2, the corresponding areal capacitances are 195.3, 145.9, 132.5, 121.1, 104.7 and 87.9 mF/cm^2. These values suggest excellent capacitive responses for ACP-120 [11].

Herein it could be well understood that carbon papers treated by potassium dichromate lotion have excellent capacitive characteristics. In general, two factors, specific surface area and surface hydrophilicity, have been considered count for activated carbon papers as supercapacitor electrode materials. After treatment, the surfaces of the carbon papers became rougher with enlarged specific surface areas as observed in Figs. 1 and 2. Moreover, surface hydrophilicity of activated carbon papers enhanced (shown in Fig. 4) due to hydrophilic groups such as hydroxyl (–OH), carbonyl (⟩C═O) and carboxyl (–COOH) that have been generated (shown

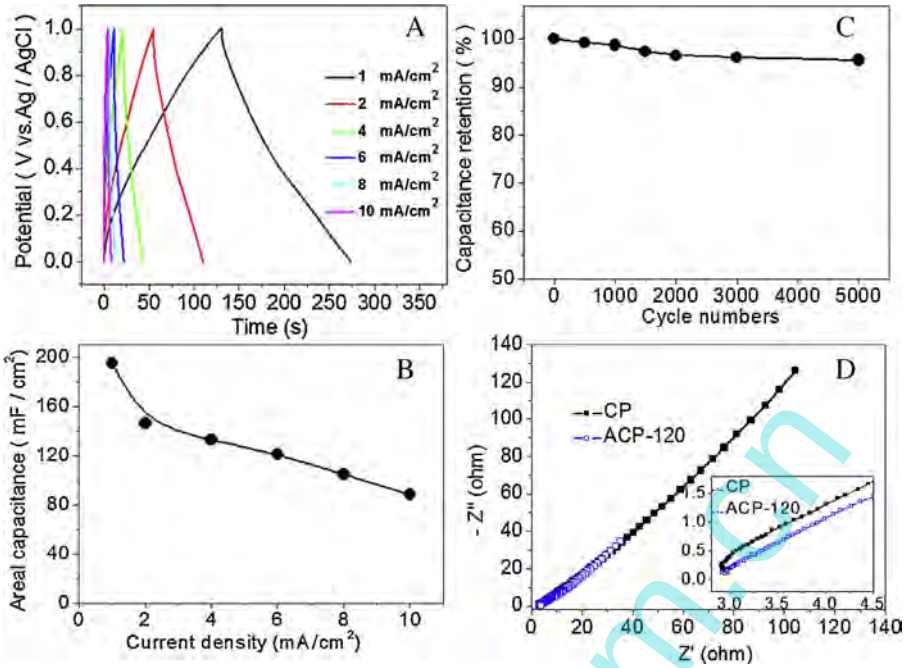

Fig. 6. (A) Charge–discharge curves at various current densities for ACP-120; (B) Areal capacitance calculated based on charge–discharge curves from plot (A) as a function of current density; (C) Capacitance retention test over 5000 cycles at a current density of 10 mA/cm^2 for ACP-120; (D) Nyquist electrochemical impedance spectra of CP and ACP-120. The inset shows a magnified view of the high frequency region of the impedance spectra.

in Fig. 3A) and they act as strong polar sites to absorb water molecules. With the synergistic effect of enlarged specific surface area and enhanced surface hydrophilicity, the activated carbon papers provide high areal capacitances.

Capacitance retention is another crucial factor for practical supercapacitors [26]. In Fig. 6C, the capacitance decay for ACP-120 over 5000 cycles is as low as 6%, implying its excellent long-term capacitive stability.

In order to further study the resistance of the supercapacitor in the double layer formation on the CP and ACP-120 electrodes, electrochemical impedance spectroscopy (EIS) were collected and shown in Fig. 6D. Only upward sloping lines in the full-scale Nyquist-type impedance spectra of CP and ACP-120 electrodes indicate that both electrodes have low diffusion resistance and exhibit good capacitive performance [27]. The inset of Fig. 6D is the magnified high-frequency region. Nearly 90° linear regions at high frequency for both CP and ACP electrodes suggest that they have the ideal capacitor behaviours [24].

4. Conclusion

In summary, we report an effective strategy using potassium dichromate lotion to activate surfaces of commercial carbon papers and accordingly enhance their capacitances. It is revealed that surfaces of activated carbon papers became rougher and their specific surface areas enlarged after treatment. Further, surface hydrophilicity of activated carbon papers enhanced due to the generation of hydrophilic groups such as hydroxyl (–OH), carbonyl (⟩C═O) and carboxyl (–COOH) and they act as strong polar sites to absorb water molecules. With the synergistic effect of enlarged specific surface area and enhanced surface hydrophilicity, the activated carbon papers provide high areal capacitances. Meanwhile, the capacitance decay for ACP-120 over 5000 cycles is as low as 6%, implying its excellent long-term capacitive stability. The EIS results indicate that CP and ACP electrodes have low diffusion resistance and exhibit good capacitive performance. In general, our strategy offers a feasible pathway to make commercial carbon paper a promising candidate for practical supercapacitors and can be extended to other carbon based electrode materials.

Acknowledgements

The work described in this paper was supported by the National Natural Science Foundation of China (No. 51206029) and Foundation for the Excellent Young Teachers in Higher Education Institutions of Guangdong (Yongfu Qiu, 2014). We thank Qiu Yan (1941308558@qq.com) for her linguistic assistance during the preparation of this manuscript.

References

[1] Y.W. Zhu, S. Murali, M.D. Stoller, K.J. Ganesh, W.W. Cai, P.J. Ferreira, A. Pirkle, R.M. Wallace, K.A. Cychosz, M. Thommes, D. Su, E.A. Stach, R.S. Ruoff, Carbon-based supercapacitors produced by activation of graphene, Science 332 (2011) 1537–1541.
[2] X. Peng, L.L. Peng, C.Z. Wu, Y. Xie, Two dimensional nanomaterials for flexible supercapacitors, Chem. Soc. Rev. 43 (2014) 3303–3323.
[3] G.P. Wang, L. Zhang, J.J. Zhang, A review of electrode materials for electrochemical supercapacitors, Chem. Soc. Rev. 41 (2012) 797–828.
[4] X.L. Chen, H.J. Lin, P.N. Chen, G.Z. Guan, J. Deng, H.S. Peng, Smart, stretchable supercapacitors, Adv. Mater. 26 (2014) 4444.
[5] Y. Yang, Z.W. Peng, G.N. Wang, R.D. Ruan, X.J. Fan, L. Li, H.L. Fei, R.H. Hauge, J.M. Tour, Three-dimensional thin film for lithium-ion batteries and supercapacitors, ACS Nano 8 (2014) 7279–7287.
[6] X.L. Yan, X.J. Li, Z.F. Yan, S. Komarneni, Porous carbons prepared by direct carbonization of MOFs for supercapacitors, Appl. Surf. Sci. 308 (2014) 306–310.
[7] B.J. Jiang, C.G. Tian, L. Wang, L. Sun, C. Chen, X.Z. Nong, X.J. Qiao, H.G. Fu, Highly concentrated, stable nitrogen-doped graphene for supercapacitors: simultaneous doping and reduction, Appl. Surf. Sci. 258 (2012) 3438–3443.
[8] Y. Qiu, Z. Cheng, B. Guo, H. Fan, S. Sun, T. Wu, L. Jin, L. Fan, X. Feng, Preparation of activated carbon paper through a simple method and application as a supercapacitor, J. Mater. Sci. 50 (2015) 1586–1593.
[9] Y. Qiu, P. Xu, B. Guo, Z. Cheng, H. Fan, M. Yang, X. Yang, J. Li, Electrodeposition of manganese dioxide film on activated carbon paper and its application in supercapacitors with high rate capability, RSC Adv. 4 (2014) 64187–64192.
[10] L.L. Zhang, X.S. Zhao, Carbon-based materials as supercapacitor electrodes, Chem. Soc. Rev. 38 (2009) 2520–2531.

[11] Y.Y. Horng, Y.C. Lu, Y.K. Hsu, C.C. Chen, L.C. Chen, K.H. Chen, Flexible supercapacitor based on polyaniline nanowires/carbon cloth with both high gravimetric and area-normalized capacitance, J. Power Sources 195 (2010) 4418–4422.
[12] B. Xu, S.F. Yue, Z.Y. Sui, X.T. Zhang, S.S. Hou, G.P. Cao, Y.S. Yang, What is the choice for supercapacitors: graphene or graphene oxide? Energy Environ. Sci. 4 (2011) 2826–2830.
[13] L.B. Hu, M. Pasta, F. La Mantia, L.F. Cui, S. Jeong, H.D. Deshazer, J.W. Choi, S.M. Han, Y. Cui, Stretchable, porous, and conductive energy textiles, Nano Lett. 10 (2010) 708–714.
[14] J. Yan, Z.J. Fan, T. Wei, J. Cheng, B. Shao, K. Wang, L.P. Song, M.L. Zhang, Carbon nanotube/MnO_2 composites synthesized by microwave-assisted method for supercapacitors with high power and energy densities, J. Power Sources 194 (2009) 1202–1207.
[15] B. Sun, M. Skyllas-Kazacos, Chemical modification of graphite electrode materials for vanadium redox flow battery application-part II. Acid treatments, Electrochim. Acta 37 (1992) 2459–2465.
[16] A.G. Osorio, I.C.L. Silveira, V.L. Bueno, C.P. Bergmann, H_2SO_4/HNO_3/HCl-functionalization and its effect on dispersion of carbon nanotubes in aqueous media, Appl. Surf. Sci. 255 (2008) 2485–2489.
[17] C.T. Hsieh, H. Teng, W.Y. Chen, Y.S. Cheng, Synthesis, characterization, and electrochemical capacitance of amino-functionalized carbon nanotube/carbon paper electrodes, Carbon 48 (2010) 4219–4229.
[18] Y.F. Qiu, L. Wang, C.F. Leung, G.J. Liu, S.H. Yang, T.C. Lau, Preparation of nitrogen doped $K_2Nb_4O_{11}$ with high photocatalytic activity for degradation of organic pollutants, Appl. Catalysis A: Gen. 402 (2011) 23–30.
[19] D. Yang, A. Velamakanni, G. Bozoklu, S. Park, M. Stoller, R.D. Piner, S. Stankovich, I. Jung, D.A. Field, C.A. Ventrice, R.S. Ruoff, Chemical analysis of graphene oxide films after heat and chemical treatments by X-ray photoelectron and Mircro-Raman spectroscopy, Carbon 47 (2009) 145–152.
[20] A. Barinov, O.B. Malciglu, S. Fabris, T. Sun, L. Gregoratti, M. Dalmiglio, M. Kiskinova, Initial stages of oxidation on graphitic surface: photoemission study and density functional theory calculations, J. Phys. Chem. C 113 (2009) 9009–9013.
[21] T.S. Chow, Wetting of rough surfaces, J. Phys.: Condens. Matter 10 (1998) L445–L451.
[22] C.K. Söz, E. Yilgör, I. Yigör, Influence of the average surface roughness on the formation of superhydrophobic polymer surfaces through spin-coating with hydrophobic fumed silica, Polymer 62 (2015) 118–128.
[23] N. Giovambattista, P.G. Debenedetti, P.J. Rossky, Effect of surface polarity on water contact angle and interfacial hydration structure, J. Phys. Chem. B 111 (2007) 9581–9587.
[24] Z. Gui, H.L. Zhu, E. Gillette, X.G. Han, G.W. Rubloff, L.B. Hu, S.B. Lee, Natural cellulose fiber as substrate for supercapacitor, ACS Nano 7 (2013) 6037–6046.
[25] D.H. Seo, S. Yick, S. Pineda, D. Su, G. Wang, Z.J. Han, K. Ostrikov, Single-step plasma-enabled reforming of natural precursors into vertical grapheme electrodes with high areal capacitance, ACS Sustain. Chem. Eng. 3 (2015) 544–551.
[26] Y.C. Qiu, Y.H. Zhao, X.W. Yang, W.F. Li, Z.H. Wei, J.W. Xiao, S.F. Leung, Q.F. Lin, H.K. Wu, Y.G. Zhang, Z.Y. Fan, S.H. Yang, Three-dimensional metal/oxide nanocone arrays for high-performance electrochemical pseudocapacitors, Nanoscale 6 (2014) 3626–3631.
[27] C.W. Huang, C.A. Wu, S.S. Hou, P.L. Kuo, C.T. Hsieh, H.S. Teng, Gel electrolyte derived from poly(ethylene glycol) blending poly(acrylonitrile) applicable to roll-to-roll assembly of electric double layer capacitors, Adv. Funct. Mater. 22 (2012) 4677–4685.